Single Strand DNA Specificity Analysis of Human Nucleoside Diphosphate Kinase B

Fabrice Agou, Sharona Raveh, Sébastien Mesnildrey, Michel Véron

Single Strand DNA Specificity Analysis of Human Nucleoside Diphosphate Kinase B*

Fabrice Agou, Sharona Raveh, Sébastien Mesnildrey, and Michel Véron‡

*From the Unité de Régulation Enzymatique des Activités Cellulaires, Institut Pasteur, CNRS-URA 1773,
25 rue du Docteur Roux 75724, Paris cedex 15, France*

Nucleoside diphosphate kinases (NDP kinases) form a family of oligomeric enzymes present in all organisms. Eukaryotic NDP kinases are hexamers composed of identical subunits ($\approx$17 kDa). A distinctive property of human NDPK-B encoded by the gene *nm23-H₂* is its ability to stimulate the gene transcription. This property is independent of its catalytic activity and is possibly related to the role of this protein in cellular events including differentiation and tumor metastasis. In this paper, we report the first characterization of human NDPK-B·DNA complex formation using a filter-binding assay and fluorescence spectroscopy. We analyzed the binding of several oligonucleotides mimicking the promoter region of the c-*myc* oncogene including variants in sequence, structure, and length of both strands. We show that NDPK-B binds to single-stranded oligonucleotides in a nonsequence specific manner, but that it exhibits a poor binding activity to double-stranded oligonucleotides. This indicates that the specificity of recognition to DNA is a function of the structural conformation of DNA rather than of its specific sequence. Moreover, competition experiments performed with all nucleotides provide evidence for the contribution of the six active sites in the DNA·protein complex formation. We propose a mechanism through which human NDPK-B could stimulate transcription of c-*myc* or possibly other genes involved in cellular differentiation.

Nucleoside diphosphate kinases are essential oligomeric enzymes that play a key role in the maintenance of the intracellular pool of all (d)NTPs and NTPs. They catalyze the transfer of a phosphate from a nucleoside triphosphate to a nucleoside diphosphate via the formation of an enzymatic intermediate phosphorylated on a catalytic histidine residue (1). The crystal structures of NDP[1] kinases from several organisms including prokaryotes (2) and eukaryotes (3–5) have been determined. They all share a common subunit fold, built around a $\beta\alpha\beta\beta\alpha\beta$ motif, also present in the "palm domain" of DNA polymerases (5). Although the prokaryotic enzyme from *Myxococcus xanthus* is a tetramer (6), all eukaryotic enzymes known to date are hexamers composed of identical subunits each containing an active site. The hexameric state is essential for enzymatic

activity, and binding of ADP or ATP contribute to the hexamer stability (7).

In human cells, four members of the NDP kinase family encoded by the genes *nm23-H₁* (8), *nm23-H₂* (9), *DR-nm23* (10), and *nm23-H₄* (11) have been identified so far. A fifth isoform, *nm23-H₅* was isolated very recently but it does not exhibit NDP kinase activity when overexpressed in bacteria (12). Nm23-H₁ and Nm23-H₂ share the highest homology (88%) and can form heterohexamers (13). Nm23-H₂/NDPK-B is present both in the cytoplasm and in the nucleus (14, 15). Phylogenetic analysis (16) and GFP fusion-protein constructs[2] indicate that Nm23-H₄ is a mitochondrial form of NDP kinase. Altered levels of expression of *nm23-H₁*, *nm23-H₂* and *DR-nm23* are associated with a variety of cellular processes including differentiation, proliferation, apoptosis, and suppression of tumor metastasis (17). Using the serial analysis of gene expression method (18), it was shown that *nm23-H₂* was up-regulated in gastrointestinal tumors (19). Remarkably, the catalytic activity does not explain the role of *nm23* in these cellular processes (17, 20, 21).

A role for the *nm23-H₂* gene product in cell regulation independent from its NDPK activity was first suggested by the observation that this protein binds to nucleic acids. Indeed NDPK-B was identified as a transcription factor based on its ability to stimulate the transcription *in vitro* of the c-*myc* gene (22). This stimulatory activity is independent from the enzymatic activity, because it was retained in a catalytically inactive mutant (23). In addition, transient transfections of a plasmid bearing the $-160/-101$ upstream nuclease hypersensitive element of the c-*myc* promoter (also termed PuF site or CT element), have shown that NDPK-B increases the expression of a reporter gene by 3–5-fold (24, 25). Moreover, mutations in the PuF site affect the transcriptional efficiency of NDPK-B (25). However Michelotti *et al.* (26) using a one-hybrid system, showed that NDPK-B is not a conventional transcription factor. The nuclease hypersensitive element contains a sequence homopurine/homopyrimidine-rich, which is prone to form non-B duplex DNA-like intermolecular triplexes (27, 28) or tetraplexes (29). This region is nucleosome-free (30) and forms single strand DNA (31), presumably resulting from the appearance of secondary structure. Using a mobility shift assay, we reported previously a qualitative analysis of the DNA-binding properties of NDPK-B (32), indicating a preference for single strand binding.

In this study, we report the first quantitative analysis of human NDPK-B·DNA complex formation using several biochemical methods. We show that NDPK-B binds to single-stranded oligonucleotides in a nonsequence specific manner, but that it exhibits strong specificity for single-stranded DNA. Moreover, competition experiments performed with NDPs show that the affinity for DNA is significantly higher than for

nucleosides di- and triphosphates, and provide evidence that the six active sites of the hexamer form a binding template for the interaction with oligonucleotides. We propose a mechanism through which human NDPK-B could stimulate transcription of c-*myc* and possibly of other genes involved in cellular differentiation.

EXPERIMENTAL PROCEDURES

Materials and Preparation of the Oligonucleotides

The oligonucleotides were purchased from Genset or Pasteur Institute. All NDPs and GTP were obtained from Roche Molecular Biochemicals. T4 polynucleotide kinase was purchased from New England Biolabs.

All oligonucleotides were gel-purified following protocols derived from Sambrook *et al.* (33). The elution buffer was 0.3 M sodium acetate, pH 7, and 1 mM EDTA. The short oligonucleotides (10 polymers) were precipitated out of the solution in dry ice using an ethanol/isopropanol (4:1 v/v) mixture, which improved the recovery of precipitation. The pellet was washed twice with 95% ethanol and resuspended in water. Concentrations of single strand and double strand oligonucleotides were measured by absorbance at 260 nm according to the nearest neighbor approximations of Puglisi and Tinoco (34) for single strand and using an extinction coefficient of 1.68×10^4 M base pair$^{-1} \times$ cm^{-1} for double strand.

Purification of Human NDPK-B Expressed in Escherichia coli

The expression vector pJC20 containing the complete coding sequence of the *nm23-H₂* cDNA was a gift from Dr. M. Konrad (Max Planck Institute for Biophysical Chemistry, Göttingen). Expression of human NDPK-B was induced by addition of 1 mM isopropyl-1-thio-β-D-galactopyranoside for 5 h when the culture (5 liters) reached a cell density of $A_{600\ nm} \approx 0.5$. After harvesting by centrifugation, the cells were washed twice and resuspended in extraction buffer (10 mM potassium phosphate, pH 7.5, 5% glycerol, 1 mM EDTA, 5 mM magnesium chloride, and 1 mM DTE) containing protease inhibitors. Cells were broken in a French press at 1,500 p.s.i. The lysate was diluted 2.5-fold with extraction buffer and centrifuged at $10,000 \times g$ for 20 min. All subsequent steps were performed at 4 °C. Following precipitation of nucleic acids by addition of Polymin P (BASF) at 0.15% (v/v) and centrifugation at $10,000 \times g$ for 15 min, the clear supernatant (162 ml) was applied to a POROS HQ column (PerSeptive Biosystems, 2.6×12 cm), equilibrated in 50 mM Tris-HCl, pH 8, 5% glycerol and 1 mM DTE. The recombinant NDPK-B was recovered in the flow-through fraction and was separated from the endogenous NDP kinase from *E. coli*, which binds to the matrix. Fractions containing NDP kinase activity were pooled (174 ml) and applied to a POROS HS (1.6×16 cm) equilibrated in 25 mM potassium phosphate, pH 7.5, 1 mM EDTA, 5% glycerol, and 1 mM DTE, and eluted with a 650-ml linear gradient of potassium phosphate (25–400 mM). Protein-containing fractions according to the optical density profile at 280 nm were pooled (45 ml), applied on a ceramic hydroxyapatite column (American International Chemical, 1.6×10 cm), equilibrated in 25 mM potassium phosphate, 5% glycerol, and 1 mM DTE and eluted with a 520-ml linear gradient of potassium phosphate (25–400 mM). Fractions containing NDPK-B were concentrated, and the excess salt removed by ultrafiltration (Amicon). The protein sample was then dialyzed against 25 mM potassium phosphate, pH 7.5, 2 mM DTE, and 50% glycerol, and stored at −20 °C. The protein at this stage was >99% pure, appearing as single band after Coomassie or silver staining of a polyacrylamide gel under denaturing conditions. Protein concentration was determined either by the method of Bradford or by absorbance at 280 nm using an extinction coefficient of 1.238 for a 1 mg/ml solution. NDP kinase activity was assayed by a coupled assay using 0.2 mM dTDP as the phosphate acceptor in the presence of 1 mM ATP as described (35). The specific activity of pure NDPK-B was 1,400 units/mg (1 unit corresponds to the amount of dTDP (micromoles) transformed/min at 25 °C). A summary of the purification protocol is shown in Table II.

Detection of NDPK-B·Oligonucleotide Complexes

Filter-binding Assay—All oligonucleotides used in filter-binding experiments (see Table I) were radiolabeled with [γ-³²P]ATP by T4 polynucleotide kinase. Radiolabeled oligonucleotides were separated from free [γ-³²P]ATP on denaturing polyacrylamide gels. Labeled oligonucleotides were incubated with NDPK-B in a 30-μl total volume of binding buffer at pH 5.5 (FS buffer, 20 mM Tris/acetic acid/MES, 20% glycerol, 5 mM magnesium chloride, and 1 mM DTE) or at a different pH

TABLE I
c-myc DNA promoter region and oligonucleotides used in this study

The hypersensitive sites to DNase I (◆, site III₁) or nuclease S1 (▼) are indicated on the c-*myc* DNA sequence relative to the P1 transcription start site (49). Bases that show protection *in vivo* after treatment with DMS (25) are indicated by an asterisk and those protected *in vitro* by the complex DNA·NDPK-B are underlined (25, 43). AML represents the initiator region of the adenovirus major late promoter from −12 to +18.

```
−153                          ◆        ▼▼−110
5′TCTCCTCCCCACCTTCCCCACCCTCCCCACCCTCCCCATAAGCG  3′
 AGAGGAGGGGTGGAAGGGGTGGGAGGGGTGGGAGGGGTATTCGC
        *** *** **** ***
```

Oligonucleotide	Length	Sequence(5′→3′)
c-*myc*/ssPu-29	29	ATGGGGGAGGGTGGGGAGGGTGGGGAAGGT
c-*myc*/ssPy-30	30	CACCTTCCCCACCCTCCCCACCCTCCCCAT
c-*myc*/ssPu-10	10	TGGGGAGGGT
c-*myc*/ssPy-10	10	ACCCTCCCCA
d(CT)₉	18	CTCTCTCTCTCTCTCTCT
d(CT)₂₇	54	CT . . . (CT)₂₅ . . . CT
AML/ssPu-30	30	CGCAAGCAGGAGTGAGAGAAGGCGTAGCAC
AML/ssPy-30	30	GTGCTACGCCTTCTCTCACTCCTGCTTGCG
dAdG	2	AG

for 30 min at 4 °C. Reaction mixtures were passed through a nitrocellulose membrane (0.45 μm pore size, Millipore HA filters) under reduced pressure in a cold room. Before sample application, the filter was pretreated with 0.5 ml of the FS buffer containing 1 mg/ml bovine serum albumin. After application of the samples, the filters were washed twice with 0.5 ml of FS buffer containing, 20, 50, 100, or 200 mM potassium chloride. The filters were then dried and counted by liquid scintillation. The filter efficiency (*E*) was determined from Equation 1,

$$E = \frac{C_S - C_B}{C_T - C_B} \qquad \text{(Eq. 1)}$$

where C_S represents the counts retained on the filter when the oligonucleotides are saturated with NDPK-B (NDPK-B $\to \infty$), C_B represents the background counts obtained when the oligonucleotide is filtered without NDPK-B and C_T is the total input counts.

Ionic Strength Dependence of Complex Formation

The salt dependence of the binding of NDPK-B to the oligonucleotide was determined by conducting titration experiments in FS buffer and washing buffer at pH 5.5 with different potassium chloride concentrations. The effect of the salt concentration on complex formation has been described by the relation (36),

$$\frac{-\partial \ln K_D}{\partial \ln[K^+]} = -m' \cdot \psi \qquad \text{(Eq. 2)}$$

where m' is the number of ion pairs formed and Ψ is the fraction of counterion bound per phosphate group, which is assumed to be 0.71 (36). Assuming that m' is equivalent to N, the number of ion pairs, the non-electrostatic contributions to the free energy of binding (ΔG^0_{ne}) has been estimated according to Equation 3,

$$\Delta G^0_{ne} = \Delta G^0_{obs}(1\ \text{M}\ K^+) - N\Delta G^0_{Lys} \qquad \text{(Eq. 3)}$$

where ΔG^0_{obs} is the standard free energy at $[K^+] = 1$ M, ΔG^0_{Lys} is the standard free energy of formation of a single lysine-phosphate ionic interaction and corresponds to ≈ 0.18 kcal·mol^{-1} at $[K^+] = 1$ M (36, 37).

Competition Experiments—To measure the effect of NDP on NDPK-B/oligonucleotide binding, competition experiments were performed. The oligonucleotide c-*myc*/ssPu-30 (70 nM), radiolabeled with [γ-³²P]ATP was incubated at 4 °C with NDPK-B (120 nM) in FS buffer. Variable amounts of NDP (10 nM $\to$ 5 μM) were then added (final volume; 30 μl). After binding was complete (30 min), the samples were filtered and washed with 2×500 μl washing buffer (FS) containing 20 mM potassium chloride. Using mass balance and equilibrium binding equations, the equilibrium mixture of γ-³²P-oligonucleotide (DNA) and competitor NDP (*I*) binding to NDPK-B (*P*) can be described by Equation 4,

$$\frac{[\text{DNA}\cdot\text{P}]}{[\text{DNA}]_\text{T}} = K_D(1 + ([I]/K_I)) + [\text{DNA}]_\text{T} + [\text{P}]_\text{T} -$$

$$\sqrt{K_D(1 + ([I]/K_I)) + [\text{DNA}]_\text{T} + [\text{P}]_\text{T} - 4\cdot[\text{DNA}]_\text{T}\cdot[\text{P}]_\text{T}}/2\cdot[\text{DNA}]_\text{T} \quad \text{(Eq. 4)}$$

TABLE II
Purification of recombinant NDPK-B

All purification steps were performed at 4 °C. One unit of activity corresponds to the amount of dTDP (micromoles) transformed/min at 25 °C.

Purification step	Total protein	Total activity	Specific activity	Yield	Relative purification factor
	mg	*units*	*units/mg*	*%*	
Crude extract	2,855	195,500	69	100	1
Polymin-P supernatant	1409	182,250	130	93	2
POROS HQ	487	169,650	348	87	5
POROS HS	90	118,215	1,314	61	19
Ceramic hydroxyapatite	60	84,000	1,400	43	20

where $[DNA]_T$, $[P]_T$ are the total concentration of the radiolabeled oligonucleotide and NDPK-B, respectively, and I is the free concentration of inhibitor NDP, which in our conditions is very close to the total concentration. K_D is the dissociation constant for the DNA-NDPK-B interaction and K_I is the inhibition constant for the NDP-NDPK-B interaction.

Fluorescence Studies—All fluorescence measurements were performed on a PTI spectrofluorometer Quantamaster™ at 20 °C, in a buffer 20 mM potassium phosphate, pH 7.0, containing 75 mM potassium chloride, 5% glycerol, 5 mM magnesium chloride, and 1 mM DTE. The excitation wavelength was 304 nm to minimize the contribution of tyrosyl residues to the total fluorescence and the inner filter due to light absorption by the oligonucleotide. Protein fluorescence was measured at 340 nm and the excitation and emission bandwidths were both set to 2.5 nm. The oligonucleotide titrations were carried out with NDPK-B monomeric concentrations of 0.5–2 μM (1 ml) by adding varying amounts of DNA to a constant concentration of NDPK-B. In all titration experiments, the progressive dilution during the course of titration never exceeded 5%. Following the addition of the saturating oligonucleotide concentration, the equilibrium state was checked by recording the protein fluorescence during 5 min. In the fluorescence titrations each reading was collected for 60 s after a 1-min period of equilibration. The extent of photobleaching was determined by performing experiments without adding the oligonucleotide. The decrease in fluorescence due to photobleaching is less than 0.6% in a 15-point titration.

Calculation of Binding Parameters—Bimolecular binding data were fitted to the Langmuir binding equation. The independent variable in these experiments was either total oligonucleotide or total NDPK-B concentrations. The equation was then converted to a function of total NDPK-B and total oligonucleotide for fluorescence experiments (Eq. 5);

$$[DNA \cdot P] = K_D + [DNA]_T + n[P]_T$$
$$- \sqrt{K_D + [DNA]_T + n[P]_T - 4[DNA]_T n[P]_T} = A \quad (Eq.\ 5)$$

where K_D represents the dissociation constant, $[P]_T$ is the total NDPK-B concentration, n is the number of equivalent binding sites, and $[DNA]_T$ is the total oligonucleotide concentration (a similar scheme can be worked out for titration of DNA by NDPK-B using the filter-binding assay; $[DNA]_T$ is substituted for $n[DNA]_T$ and $n[P]_T$ for $[P]_T$). For fluorescence experiments, because the quenching was directly proportional to binding, the theoretical quenching was $F_{obs} = (F_0 - F_{max}) \cdot A' + F_0$ (Eq. 5') where F_0 is the initial fluorescence intensity before addition of the oligonucleotide, F_{max} is the fluorescence after saturation with the oligonucleotide, and A' is the molar fraction of protein site occupied. In the filter-binding assay, the fraction of oligonucleotide retained on a filter, R, was calculated as follows: $(C - C_B)/(C_T - C_B)$ where C is the counts retained on the filter, C_B is the counts obtained in the absence of NDPK-B, and C_T is the total input counts. Experimental data were fitted according to the symmetric equation derived from Equation 5, including the filter efficiency, E, as follows: $R = E \cdot A''$ where A'' is the molar fraction of oligonucleotide bound. All experimental data were fitted by nonlinear regression analysis using the Levenberg-Marquardt algorithm in the commercially available graphics software package KaleidaGraph (Synergy Software, Reading PA). For fluorescence experiments, because it is hazardous to fit the experimental data with two parameters estimated (n and K_D), we determined graphically the stoichiometry n using a NDPK-B concentration (2 μM) higher than the K_D expected, such that the abscissa of the intersection between the initial tangent and the asymptote is practically equal to $n \cdot [NDPK-B]_T$. Then, the K_D was calculated by fitting the equation (Eq. 5') using a NDPK-B concentration of 0.5 μM.

Analytical Ultracentrifugation—Sedimentation equilibrium experiments were performed at 9,000, 12,000, 16,000, and 18,000 rpm at 15 or 10 °C in a Beckman Optima XL-A analytical ultracentrifuge, using an An-60 Ti rotor and a double-sector cell of 12-mm path-length. Enzyme samples (400 μl) were dialyzed exhaustively against three changes of buffer (500 ml each) described in Table III. Equilibrium was verified from the superimposition of duplicate scans recorded at 3 h intervals. The experimental data were first fitted to a model for a single homogeneous species following Equation 6 (38),

$$c_{(r)} = c_{(ref)} \exp\{[(M(1 - \bar{v}\rho)\omega^2/2\,RT](r^2 - r_{ref}^2)\} + \delta \quad (Eq.\ 6)$$

where $c_{(r)}$ is the concentration of the protein at radial position r, $c_{(ref)}$ is the concentration of the protein at an arbitrary reference distance r_{ref}, M is the molecular mass, $\bar{v}$ is the partial specific volume of the solute, ρ is the density of the solvent, ω is the angular velocity, R and T are the molar gas constant and the absolute temperature, respectively, and δ is the base-line offset. The partial specific volume was calculated from the amino acid composition of the protein, and the density of the buffers was determined from published tables (38). After collecting data at sedimentation equilibrium, samples were centrifuged at 40,000 rpm for 12 h to sediment the protein, and radial scans were again collected to obtain a base-line correction for each cell. In all cases, because inclusion of a second virial coefficient gave no improvement of the fit, nonideality in the system was not detected.

RESULTS

Purification of Recombinant NDPK-B—Because human NDPK-B is a basic protein, its ability to bind nucleic acids in cellular extracts could interfere with the purification process. Indeed, the protein obtained using the previous purification procedure (32, 39) was contaminated by nucleic acids. We developed a new purification method including a precipitation of the nucleic acids with Polymin-P, followed by three ion-exchange chromatography steps (see Table II). It should be noted that, despite Polymin-P precipitation and the passage on a strong anion-exchanger (POROS HQ), nucleic acids were still present in the flow-through fraction containing NDP kinase activity, as shown by the absorption spectrum of the protein. Two additional steps on cation-exchanger columns with extensive washing, were necessary to obtain a pure protein free from nucleic acids as judged from SDS-polyacrylamide gel electrophoresis stained by silver nitrate and from the shape of the absorption spectra (data not shown).

Oligomeric State of Recombinant NDPK-B—A tetrameric structure was recently reported for human recombinant NDPK-B expressed in *E. coli* (39). However, the crystal structure of NDPK-B (5, 40) showed that its oligomeric state is α_6. We previously demonstrated that DNA binding to the *Dictyostelium* enzyme is strongly dependent on its oligomeric state. Indeed, while a dimeric mutant from *Dictyostelium* binds to a single strand oligonucleotide, the hexameric wild-type does not (41). We checked the oligomeric state of our purified recombinant NDPK-B by equilibrium sedimentation. Fig. 1 shows the experimental distribution at 12,000 rpm under buffer conditions used by Schaertl (39). The relative concentration of NDPK-B was fitted to an ideal monodisperse solute of $105,000 \pm 3,000$ (Table III). Considering that the initiator methionine is removed by methionine aminopeptidase (39, 42), this value precisely matches the theoretical calculated mass of the hexameric species 103,002 Da (6×17, 167 Da). The distribution of NDPK-B, obtained at two other rotor speeds (9,000

FIG. 1. **Sedimentation equilibrium analysis of NDPK-B.** Relative concentration of NDPK-B measured by absorbance at 280 nm is plotted as a function of radial distance after sedimentation under the conditions described in Table III at 12,000 rpm. Experimental values (○) were fitted (*curve*) as described under "Experimental Procedures." The line shows the best-fitting curve for an ideal monospecies with a molecular mass equivalent to 105,000 Da. The distribution of residuals is shown above.
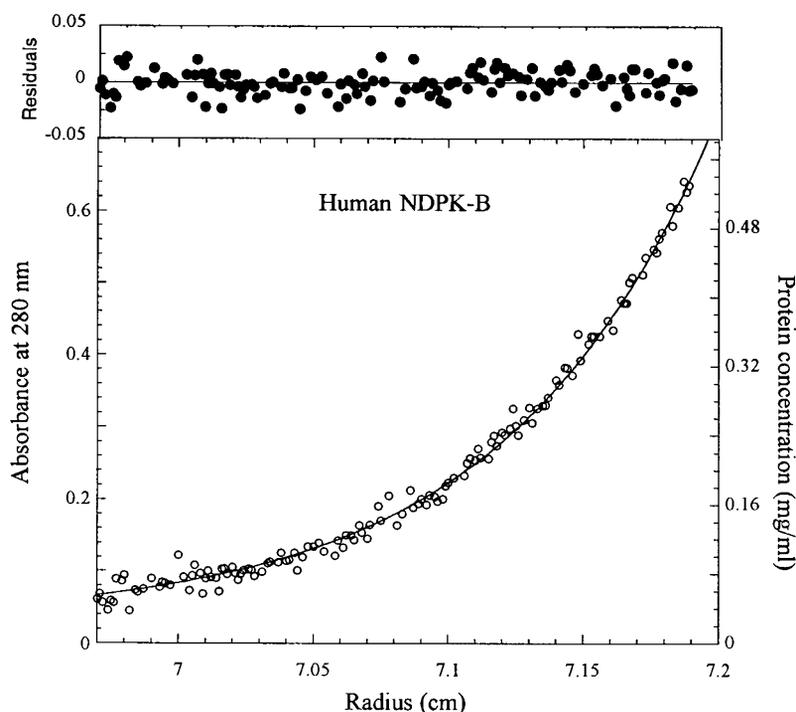
TABLE III
Sedimentation equilibrium analysis of human NDPK-B

Experimental conditions were similar to those used by (39). Molecular masses were obtained by fitting Equation 6 described under "Experimental Procedures" in a single ideal solute model. The enzyme behaved as a monodispers entity in each of the runs.

Buffer	Temperature	Initial protein concentration	Speed	Molecular mass observed	Molecular species
	°C	*mg/ml*	*rpm*	*Da*	*%*
50 mM Tris-HCl, pH 8			9,000	97,000 ± 8,000	100 α_6
5 mM MgCl$_2$					
1 mM EDTA	15	0.2	12,000	105,000 ± 3,000[a]	100 α_6
100 mM KCl					
1 mM DTE			18,000	100,000 ± 4,000	100 α_6
10 mM MES, pH 6.0					
5 mM MgCl$_2$	10	0.2	16,000	106,000 ± 6,000	100 α_6
1 mM DTE					

[a] The sedimentation profile of human NDPK-B is shown in Fig. 1.

and 18,000 rpm) could also be fitted to a single ideal homogeneous species with a molecular mass corresponding to a hexamer (Table III), indicating that no dissociated form could be detected in our enzymatic preparation. The stability of the hexameric protein was also examined. Lowering the temperature to 10 °C and removing KCl in a more acidic buffer, pH 6, did not alter the oligomeric structure (Table III).

Characterization of the NDPK-B·Single Strand DNA Complex—We first quantified the interactions between NDPK-B and DNA by the filter-binding assay, a fast and simple method. We used the purine-rich single strand of the c-*myc* promoter, because it has been shown previously that most of purine bases composing this strand are protected *in vitro* by the complex DNA·NDPK-B after treatment with chemical probe (c-*myc*/ssPu-29, Table I) (25, 43). Fig. 2 shows a typical binding isotherm for the interaction of various concentrations of protein with a fixed concentration of either the c-*myc*/ssPu-29 oligonucleotide or another purine-rich strand, the AML/ssPu-30 oligonucleotide from the major late promoter of adenovirus (Table I). In each case, the shape of the binding curve is not sigmoidal, and the corresponding Scatchard plot is linear (Fig. 2, *inset*), indicating that NDPK-B binds to the oligonucleotide without cooperativity. Assuming a filter-retention efficiency of 85 and 80% for c-*myc* and AML oligonucleotides, respectively, the stoi-

chiometry of the two complexes computed from the intersection point of the two linear portions of the curve corresponds to one oligonucleotide bound per protein subunit. Taking into account this stoichiometry, the apparent K_D for c-*myc*/ssPu-29 and AML/ssPu-30 is 140 nM and 260 nM, respectively, indicating a weak preference for the c-*myc* strand as compared with the AML strand.

pH and Salt Dependence of the Binding of NDPK-B to DNA— The stability of the c-*myc*·ssPu complex with NDPK-B under several pH is shown in Table IV. The dissociation constant is 17-fold higher at pH 8.5 than at pH 5.5, indicating that at acidic pH the stability of the nucleoprotein complex is increased. At pH 5.5 or 7 and with a washing buffer at pH 5.5 (Table IV), similar K_D values (140 and 100 nM, respectively) were measured. This shows that the stability of complex retained on the filter depends essentially on the acidic pH of the washing buffer under reduced pressure. This underlines the lability of NDPK-B-single strand DNA interactions.

The KCl concentration dependence of the dissociation constant for the c-*myc*/ssPu-29 oligonucleotide was also examined (Table V). Increasing the KCl concentration from 20 to 200 mM reduces the apparent affinity by a factor of more than 50, revealing a strong contribution of the polyelectrolyte effect to the stability of the complex under our titration conditions.

FIG. 2. **Determination by the filter-binding assay of the dissociation constant of *c-myc*/ssPu-29·NDPK-B complex.** The oligonucleotide ^{32}P-c-*myc*/ssPu-29 (83 nM) or ^{32}P-AML/ssPu-30 (52 nM) was incubated with the indicated concentrations of NDPK-B under conditions described under "Experimental Procedures." *Solid curves* represent the nonlinear least-square fits using the Langmuir binding equation. *Inset*: Scatchard plot (*n/L versus n*) of the binding of c-*myc*/ssPu-30 showing a linear plot (noncooperative effect) and the stoichiometry of the oligonucleotide binding (intercept on the abscissa). Protein concentration corresponds to monomers of NDPK-B.
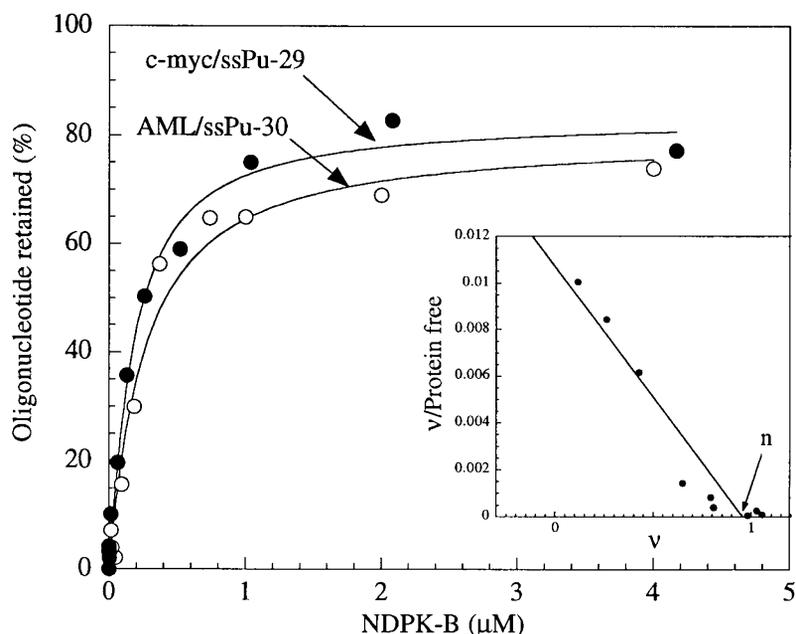
TABLE IV
pH dependence of NDPK-B binding to c-myc/ssPu-30

All assays were performed at 4 °C. Binding buffer, 20 mM Tris/acetic acid/MES containing 10 mM $MgCl_2$, 20% glycerol, and 1 mM DTE; washing buffer, same as binding buffer except for the additional presence of 20 mM KCl. The dissociation constants were measured by the filter-binding assay as described under "Experimental Procedures."

Binding buffer	Washing buffer	K_D
pH		*nM*
5.5	5.5	140 ± 30
6	6	330 ± 60
7	5.5	100 ± 10
7	7	1,600 ± 300
8	8	2,400 ± 400

TABLE V
Dependence of NDPK-B binding to c-myc/ssPu-30 on KCl concentration

All experiments were done at pH 5.5 and 4 °C in 20 mM Tris/acetic acid/MES buffer containing 10 mM $MgCl_2$, 20% glycerol, and 1 mM DTE. The dissociation constants were measured by the filter-binding assay as described under "Experimental Procedures."

[KCl]	K_D
mM	*nM*
20	140 ± 30
50	350 ± 50
100	2,600 ± 700
200	6,500[a] ± 1,000

[a] This value was estimated in a protein concentration range from 1 to 25 µM.

When the data of Table V were plotted as $-\ln[K_D]$ *versus* $\ln[KCl]$, a linear dependence of the binding on KCl concentration was found (Fig. 3). The slope of the linear regression of the data allows the calculation of the number of counterions (K^+) released from backbone phosphates upon binding of the protein (36). A value of $n = 1.73$ was obtained. Because Ψ, the fraction of a counterion bound per phosphate for single strand DNA is 0.71 (36), m' corresponding to the number of ion pairs formed between basic residues of monomeric NDPK-B and the phosphate backbone is equal to 2.4. The non-electrostatic contributions to the free energy of binding can also be estimated using Equation 3 (see "Experimental Procedures") (44). In our case, the value of ΔG^0_{obs} is about -4.0 kcal·mol^{-1} (extrapolated from the plot of $\ln[K_D]$ *versus* $\ln[K^+]$ at 1 M). Assuming that Na^+ and
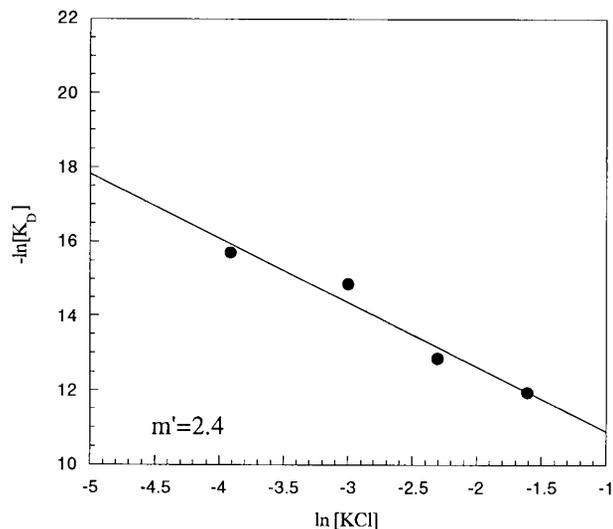

FIG. 3. **Dependence of the binding of NDPK-B to** c-*myc*/**ssPu-30 on the KCl concentration.** The oligonucleotide (80 nM) interacted with NDPK-B in buffer (20 mM Tris/Acetate/MES (pH 5.5), 10 mM $MgCl_2$, 20% glycerol, and 1 mM DTE) containing potassium chloride 20, 50, 100, and 200 mM. The data were analyzed as described under "Experimental Procedures." m' is the estimated number of ion pairs formed in the complex.

K^+ have an equivalent effect, that $\Delta G^0_{°Lys} = \Delta G^0_{Arg} = 0.18$ kcal·mol^{-1}, and that N represents the ions released (36), the non-electrostatic contributions ΔG^0_{ne} corresponds to -4.4 kcal·mol^{-1}. This indicates that under our filter-binding conditions about 50% of the total free energy is contributed by electrostatic interactions.

Competition by NDPs of the Binding of c-myc/ssPu-29 to NDPK-B—In an attempt to determine whether DNA binding involves the mono-NDP-binding site of the protein, we performed competition assays of oligonucleotide binding to NDPK-B in the presence of GDP, ADP, dTDP, or CDP. To improve the sensitivity of the competition assay, we used variable concentrations of NDP and a constant concentration of radiolabeled oligonucleotide and protein such that [NDPK-B] ≈ [oligonucleotide] ≈ K_D. As shown in Fig. 4, each of the four NDPs competed with NDPK-B binding to c-*myc*/ssPu-29. A representative fit using a quadratic equation (see Eq. 4 under
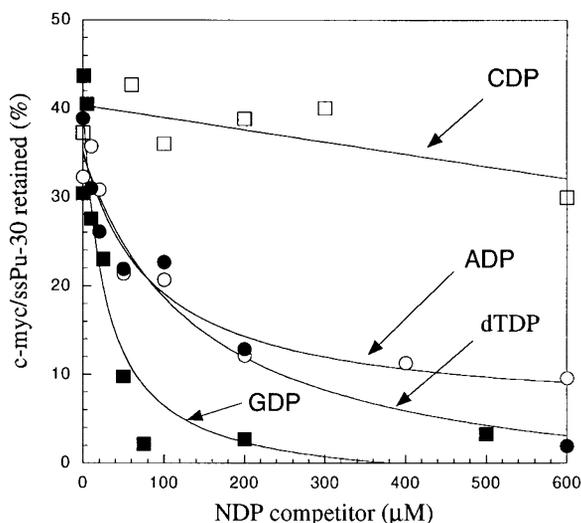
FIG. 4. **Competition by NDPs of the binding of c-*myc*/ssPu-30 to NDPK-B.** NDPK-B (120 nM, 30 μl) was incubated for 30 min at 4 °C with radiolabeled c-*myc*/ssPu-30 (70 nM) in the presence of variable concentrations of GDP (■), ADP (○), dTDP (●), or CDP (□) under the conditions described under "Experimental Procedures."

"Experimental Procedures") yielded K_I values of 17, 70, 80, and 900 μM for GDP, ADP, dTDP, and CDP, respectively. The inhibitory effect of CDP is 50-fold lower than that of GDP, demonstrating a base specificity of the inhibition. It is interesting to note that a similar base specificity has also recently been reported for the enzymatic activity of the human NDPK-B (45) and of the *Dictyostelium* enzyme (46). Moreover, analysis of the inhibition curve in the presence of GTP gives a K_I equal to 40 μM similar to that of GDP, confirming that formation of the phosphohistidine intermediate does not affect the binding of the oligonucleotide. Taken together, these results suggest strongly that the mononucleotide-binding site acts as binding template for interaction with the oligonucleotide. In addition, we show that the affinity for the best substrate, GDP, determined by stopped-flow experiments (45) is about 150-fold less than for the c-*myc*/ssPu-29.

Measurement of Affinities in Solution—To further characterize the interaction between NDPK-B and the upstream element of the c-*myc* gene, we used the filter-binding assay and fluorescence spectroscopy to determine whether NDPK-B binds to DNA with sequence specificity. Several oligonucleotides varying in sequence, structure, and length, both from the top and the bottom strands of the c-*myc* promoter, were used (Table I). Under the standard conditions described above, no complex was isolated by the filter-binding assay with pyrimidine-rich strands like c-*myc*/ssPy-30 or AML/Py-30. Similarly, only 15% of the pyrimidine strand $(CT)_9$ or 18% of $(CT)_{27}$ were retained on the filter at a saturating concentration of NDPK-B (data not shown). Because the electrostatic interactions contribute 50% of the total free energy in our filter-binding conditions as shown above, we concluded that this lability of the complex with the pyrimidine strand was probably due to the protonation of cytosine at pH 5.5. It thus appeared that the filter-binding assay was not appropriate to monitor the sequence specificity of the binding.

To measure affinities in solution, we used the fluorescence titration method to monitor the binding of oligonucleotides to NDPK-B. The measure of intrinsic protein fluorescence is the most accurate method to determine the stoichiometry of oligonucleotide binding because, contrary to the filter-binding assay, each fluorescence titration was performed using constant protein and variable oligonucleotide concentrations. Fig. 5

shows a typical emission spectrum where the excitation wavelength was 304 nm to minimize the absorptive screening effects (inner filter). The presence of a saturating concentration of c-*myc*/ssPu-29 results in a weak (5%) yet reproducible quenching of the intrinsic fluorescence of NDPK-B with no shift in the emission maximum at 348 nm. This fluorescence quenching by the oligonucleotide could be used to study the binding of various other oligonucleotides to NDPK-B.

To determine the relationship between the extent of fluorescence quenching and the fraction of protein bound, a series of fluorescence titrations with the c-*myc*/ssPy-30 pyrimidine-rich strand or c-*myc*/ssPu-29 purine-rich strand was carried out at pH 5.5 or pH 7.0 (Fig. 6 and Table VI). For these studies, we used a higher salt concentration (75 mM potassium chloride and 20 mM potassium phosphate) and a higher temperature (20 °C) to reduce the polyelectrolyte effect as described above, and to increase the hydrophobic contribution to the total free energy. Fig. 6 shows several fluorescence titrations of 30-mer oligonucleotides with NDPK-B at pH 5.5 or pH 7.0. Except with c-*myc*/ssPy-30 at pH 5.5 where the K_D is high, the stoichiometry computed from the intercept between the tangent of the initial part of the ΔF and the asymptote is equal to 1 oligonucleotide bound per 2.5 monomer. Taking this stoichiometry into account, a K_D of 35 nM was obtained at pH 5.5 for the c-*myc*/ssPu-29 strand. In contrast, the affinity of c-*myc*/ssPy-29 was very poor ($K_D > 5$ μM). This result confirms the previous filter-binding data, and indicates an excellent correlation between the fluorescence quenching and the fraction of NDPK-B bound to the oligonucleotide. No significant difference in the K_D of the c-*myc*·ssPu-29 complex was observed at pH 5.5 or pH 7, showing that binding of DNA by NDPK-B is not affected under acidic conditions. Interestingly, a K_D of 83 nM was measured at pH 7.0 with the c-*myc*/ssPy-30 pyrimidine strand. This affinity is very similar to that of the purine strand c-*myc*/ssPu29 (45 nM), indicating only a weak preference for the 29-mer c-*myc* purine-rich strand. Similar results with about 2-fold difference were obtained with shorter oligonucleotides (10-mer) purine-rich or pyrimidine-rich strands corresponding to only one repeat of the motif contained in the positive *cis*-element of the c-*myc* gene (see Table I). Thus, lowering the length of the oligonucleotide from 30- to 10-mer did not change the stoichiometry and affinity, suggesting that the main oligonucleotide/protein contacts are preserved within the 10-mer oligonucleotides. The fact that NDPK-B binds to these oligonucleotides with high but similar affinity shows that its recognition of DNA is not sequence specific. These data are further supported by the fact that another promoter (AML) displays a high affinity ($K_D = 70$ nM) for NDPK-B (Table VI). Why then does it recognize specially the upstream positive element of c-*myc* gene? To clarify this point, we measured the dissociation constant of the c-*myc* 30-mer in its double-stranded form (c-*myc*/ds-30). In contrast with single strand forms c-*myc*/ssPu-29 or c-*myc*/ssPy-30, the addition of c-*myc*/ds-30 to a constant protein concentration during fluorescence titration, generates a quenched signal which diminishes slowly as a function of time (0.2%/min), reflecting that the fluorescence titration with the double-stranded oligonucleotide is not at equilibrium. This is explained by the fact that single strand is formed from double strand in the presence of NDPK-B, as previously demonstrated using a single-strand generation assay (32). Assuming that the c-*myc*/ds-30 binding occurs very quickly under our conditions, we could estimate an apparent K_D of 5 μM for the double strand oligonucleotide, corresponding to an affinity for c-*myc*/ds-30 about 110-fold less than for the purine-rich single strand, c-*myc*/ssPu-29.

Taken together, these results suggest that specific recogni-

Fig. 5. Quenching of the fluorescence emission spectrum of NDPK-B by the c-*myc*/ssPu-29 oligonucleotide. The intrinsic fluorescence emission spectra of NDPK-B (1 μM) were recorded at 20 °C in the presence or absence of c-*myc*/ssPu-29 (2 μM) in 20 mM potassium phosphate, pH 7.0, containing 75 mM potassium chloride, 5% glycerol, 5 mM MgCl$_2$, and 1 mM DTE. The excitation wavelength was 304 nm.
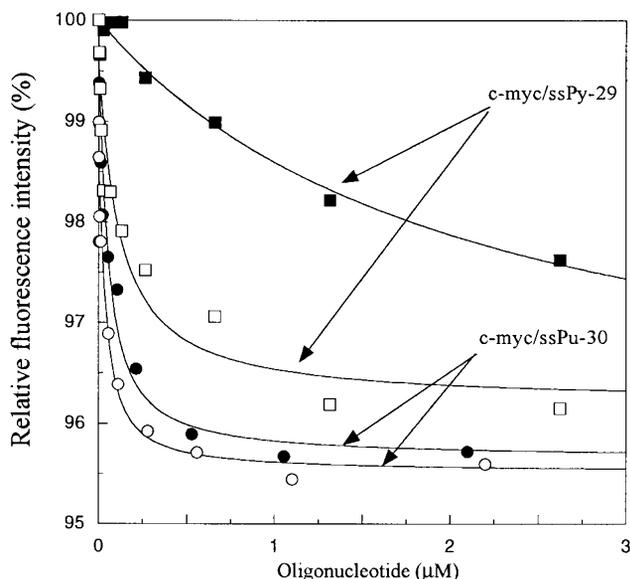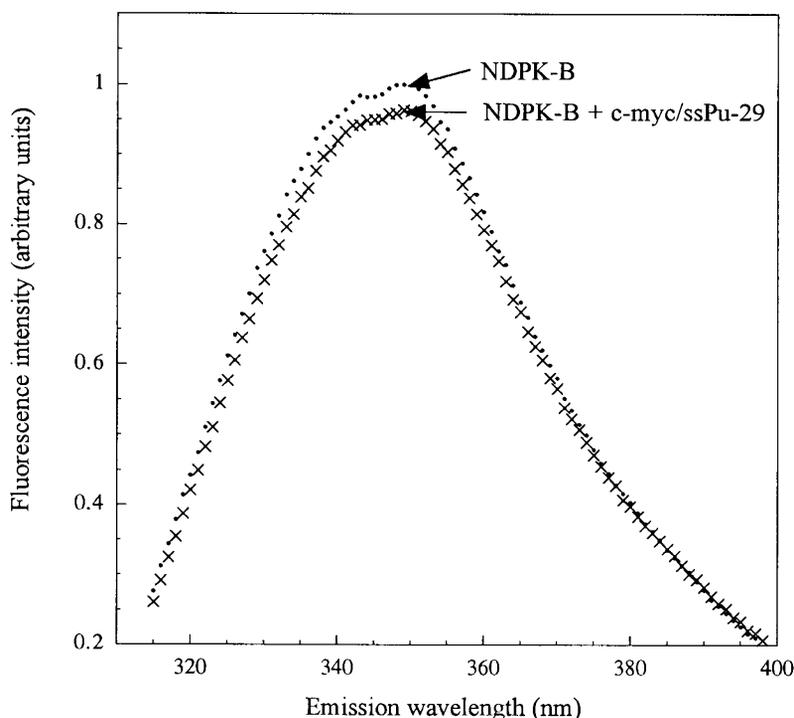

Fig. 6. Fluorescence titration of NDPK-B by c-*myc* purine-rich or pyrimidine-rich strands. Fluorescence measurements were carried out as described under "Experimental Procedures," using an excitation wavelength of 304 nm and recording the emission at 340 nm. Samples contained 20 mM KPO$_4$, pH 7.0 (○, □) or 20 mM Tris/acetic acid/MES, pH 5.5 (●, ■), 75 mM KCl, 5 mM MgCl$_2$, 5% glycerol, 1 mM DTE, 500 nM monomeric NDPK-B, and varying amounts of c-*myc*/ssPu-29 (○, ●) or c-*myc*/ssPy-30 (□, ■). The lines are the best-fit curves using Eq. 5 described under "Experimental Procedures."

tion of the upstream element of c-*myc* is essentially due to the presence of a single strand form in this DNA region rather than to base-specific contacts with the particular sequence or to a predominant homopurine/homopyrimidine composition of the stretch of DNA involved in the interaction.

DISCUSSION

In this study, two independent quantitative methods were employed to characterize the DNA-binding properties of human NDPK-B, the product of gene *nm23-H$_2$*. We found that NDPK-B binds to oligonucleotides with considerably higher

TABLE VI
Dissociation constants measured by fluorescence titration

The intrinsic fluorescence of NDPK-B was measured in the presence of several oligonucleotides in 20 mM potassium phosphate, pH 7.0, buffer or 20 mM Tris/acetic acid/MES, pH 5.5, as indicated, both containing 75 mM potassium chloride, 5% glycerol, 5 mM MgCl$_2$, and 0.5 mM DTE. Fluorescence excitation and emission wavelengths were 304 and 340 nm, respectively. Stoichiometry values presented here result from the analysis of two independent saturation curves, similar to those shown in Fig. 6, performed with 0.5 and 2 μM of NDPK-B. The stoichiometry is calculated for monomers of NDPK-B.

Oligonucleotide	K_D		Stoichiometry
	pH 5.5	pH 7	
	nM		
c-*myc*/ssPy-30	2,000 ± 200	85 ± 10	0.4
c-*myc*/ssPu-29	35 ± 7	45 ± 7	0.4
c-*myc*/ds-30	nd	5,000 ± 400	0.4
c-*myc*/ssPu-10	nd	30 ± 5	0.4
c-*myc*/ssPy-10	nd	80 ± 8	0.4
AML/ssPu-30	nd	70 ± 10	0.4

affinity as compared to its enzymatic substrates. However, different stoichiometries of the complex were observed, depending on the method and the type of titration used. In the filter-binding assay, the oligonucleotide concentration used was near the dissociation constant, conditions in which the stoichiometry could be in error (47). In contrast, a fixed protein concentration and variable oligonucleotide concentrations, such that [protein] $\gg K_D$, were used for fluorescence titration. Hence, the stoichiometry of 0.4 oligonucleotide per protein subunit derived from the fluorescence experiment is much more accurate. This corresponds to an average of 2.4 oligonucleotides bound per hexamer, assuming that the enzyme does not dissociate upon binding oligonucleotides. If the oligonucleotide binding involves the six mononucleotide binding sites as suggested by competition experiments, these results may indicate that the binding of one oligonucleotide prevents the fixation of a second strand to an adjacent protein site. It is interesting to note that a different stoichiometry (of 1:1) was observed when NDPK-B intrinsic fluorescence was titrated by dinucleotides dAdG or dGdA (data not shown), indicating that the fluorescence signal is linearly dependent on the number of bound ligands. Schnei-

der *et al.* (46) reported recently that the nucleotide analogue PAPS can adopt a new conformation inside the active site of *Dictyostelium* NDP kinase. Indeed, the 5′-phosphate of bound PAPS points out from the binding pocket, whereas the 3′-phosphate binds near the active site histidine. It is tempting to speculate that this new binding mode may also apply to the binding of an oligonucleotide to NDPK-B.

The potassium chloride dependence of NDPK-B-binding to c-*myc*/ssPu-29 shows that 2.4 ion pairs between basic residues of each monomer of NDPK-B and the phosphate backbone of the oligonucleotide contribute to the formation of the NDPK-B·DNA complex. These results are in accordance with those of Postel *et al.* (48) who showed that two strictly conserved basic residues (Arg-34 and Lys-135) are major determinants of the DNA binding.

In a previous study (32) using the mobility shift assays, we showed that NDPK-B binds preferentially single-stranded pyrimidine-rich sequences. However, this assay could be biased because of the possibility that a double strand could be generated with purine-rich (but not with pyrimidine-rich) sequences in the presence of an excess of poly(dI·dC). As shown above, the affinity for single-stranded DNA is more than 100-fold better than for a double strand, which is likely to explain why no band-shift was observed with the c-*myc*/ssPurine strand in the presence of an excess of poly(dI·dC). In this study, filter binding failed to demonstrate sequence specificity, although the acidic conditions used are appropriate to isolate protein· oligonucleotide complexes. However, such specificity is clearly demonstrated using the fluorescence method. NDPK-B binds with high affinity either poly-purine or poly-pyrimidine strands, albeit with a slight preference for the c-*myc*/purine-rich strand. This indicates that the enzyme recognizes DNA without significant sequence specificity. However, the finding that NDPK-B discriminates single strand from double strand oligonucleotides is important, and it may explain how human NDPK-B recognizes specifically the −100 to −150 upstream element of the P1 promoter (49). Indeed this element forms single-stranded DNA, according to the mapping with chemical (like KMnO$_4$) or enzymatic (like S1 nuclease) single strand probes. Other single strand DNA-binding proteins that bind to this upstream element and act on the regulation of c-*myc* expression have also been reported (50). These include the ribonucleoprotein hRNP-K, a single strand-specific transcription factor that interacts with at least two nonadjacent repeats of a cytidine-rich nonanucleotide. hRNP-K forms protein-protein interactions with components of the RNA polymerase II transcription machinery such as the TATA-binding protein (31), and its efficiency for c-*myc* gene activation is strongly dependent on the presence of single strand DNA (51). Interestingly, the specificity of NDPK-B for single strand oligonucleotides compared with double strands shown in this paper is even more pronounced than that reported for hnRNP-K (31). We propose that the transcriptional activation of c-*myc* by NDPK-B could be due to its ability to stabilize or to generate the cytosine-rich element in a single strand form to allow hnRNP-K to recognize its DNA site more efficiently. This mode of action could be related to the hexameric structure of NDPK-B containing six putative binding sites to anchor single-stranded DNA. This mechanism might be enhanced in a dimeric nuclear NDPK-B, which could be generated in tumoral cells because of an alteration of the hexameric interface. Indeed, a dimeric NDP kinase from *Dictyostelium* generated by site-directed mutagenesis has an affinity for single strand DNA 500-fold higher than for the hexameric form (41). Whereas these results were obtained by the filter-binding assay, similar evidence was also obtained using

fluorescence titration.[3] Assuming a similar behavior for human NDPK-B, an affinity for single strand equal to about 0.5 nM could be predicted and thereby would accentuate the transcriptional activation of c-*myc*.

In a more general way, the single strand specificity of DNA binding by NDPK-B demonstrated in this study could be a clue to explaining a more general role of this protein in transcription regulation. Indeed, NDPK-B could generate a single-stranded hinge in DNA that would allow the capacity of many *cis* elements to cooperate even when these elements are distant from each other. The relative abundance of NDPK-B presumably required for maintenance of the nucleoside triphosphate pool could then promote or restrict the interaction of conventional transcription factors during differentiation. An effect of NDPK-B on single-stranded DNA flexibility might also contribute to mitosis-specific single-stranded features at the promoters of active genes (52). Finally, this single-stranded specificity predicts another physiological role involved in the maintenance of discrete segments in the unwound state, which may associate the enzyme to other cellular process such as DNA recombination and replication.

REFERENCES

1. Agarwal, R. P., Robison, B., and Parks, R. E. J. (1978) *Methods Enzymol.* **51,** 376–385
2. Williams, R. L., Oren, D. A., Munoz-Dorado, J., Inouye, S., Inouye, M., and Arnold, E. (1993) *J. Mol. Biol.* **234,** 1230–1247
3. Dumas, C., Lascu, I., Morera, S., Glaser, P., Fourme, R., Wallet, V., Lacombe, M.-L., Veron, M., and Janin, J. (1992) *EMBO J.* **11,** 3203–3208
4. Chiadmi, M., Moréra, S., Lascu, I., Dumas, C., LeBras, G., Veron, M., and Janin, J. (1993) *Structure* **1,** 283–293
5. Morera, S., Lacombe, M.-L., Xu, Y., LeBras, G., and Janin, J. (1995) *Structure* **3,** 1307–131453
6. Williams, R. L., Oren, D. A., Munoz-Dorado, J., Inouye, S., Inouye, M., and Arnold, E. (1993) *J. Mol. Biol.* **234,** 1230–1247
7. Mesnildrey, S., Agou, F., Karlsson, A., Bonne, D. D., and Veron, M. (1998) *J. Biol. Chem.* **273,** 4436–4442
8. Steeg, P. S., Bevilacqua, G., Kopper, L., Thorgeirsson, U. P., Talmadge, J. E., Liotta, L. A., and Sobel, M. E. (1988) *J. Natl. Cancer Inst.* **80,** 200–204
9. Stahl, J. A., Leone, A., Rosengard, A. M., Porter, L., King, C. R., and Steeg, P. S. (1991) *Cancer Res.* **51,** 445–449
10. Venturelli, D., Martinez, R., Melotti, P., Casella, I., Peschle, C., Cucco, C., Spampinato, G., Darzynkiewicz, Z., and Calabretta, B. (1995) *Proc. Natl. Acad. Sci. U. S. A.* **92,** 7435–7439
11. Milon, L., Rousseau-Merck, M., Munier, A., Erent, M., Lascu, I., Capeau, J., and Lacombe, M. (1997) *Hum. Genet.* **99,** 550–557
12. Munier, A., Feral, C., Milon, L., Phung-Ba Pinon, V., Gyapay, G., Capeau, J., Guellaen, G., and Lacombe, M. L. (1998) *FEBS Lett.* **434,** 289–294
13. Gilles, A. M., Presecan, E., Vonica, A., and Lascu, I. (1991) *J. Biol. Chem.* **266,** 8784–8789
14. Kraeft, S., Traincard, F., Bourdais, J., Mesnildrey, S., Veron, M., and Chen, L. B. (1996) *Exp. Cell Res.* **227,** 63–69
15. Pinon, V. P. B., Millot, G., Munier, A., Vassy, J., Linares-Cruz, G., Capeau, J., Calvo, F., and Lacombe, M. L. (1999) *Exp. Cell Res.* **246(2),** 355–367
16. Lambeth, D. O., Mehus, J. G., Ivey, M. A., and Milavetz, B. I. (1997) *J. Biol. Chem.* **272,** 24604–24611
17. De La Rosa, A., Williams, R. L., and Steeg, P. S. (1995) *BioEssays* **17,** 53–62
18. Velcolescu, V. E., Zhang, L., Vogelstein, B., and Kinzler, K. W. (1995) *Science* **270,** 484–487
19. Zhang, L., Zhou, W., Velcolescu, V., Kern, S., Hruban, R., Hamilton, S., Vogelstein, B., and Kinzler, K. (1997) *Science* **276,** 1268–1272
20. Xu, J., Liu, L. Z., Deng, X. F., Timmons, L., Hersperger, E., Steeg, P., Veron, M., and Shearn, A. (1996) *Dev. Biol.* **177,** 544–557
21. Sastre-Gareau, X., Lacombe, M.-L., Jouve, M., Veron, M., and Magdelenat, H. (1992) *Int. J. Cancer* **50,** 533–538
22. Postel, E. H., Berberich, S. J., Flint, S. J., and Ferrone, C. A. (1993) *Science* **261,** 478–480
23. Postel, E. H., and Ferrone, C. A. (1994) *J. Biol. Chem.* **269,** 8627–8630
24. Berberich, S. J., and Postel, E. H. (1995) *Oncogene* **10,** 2343–2347
25. Ji, L., Arcinas, M., and Boxer, L. M. (1995) *J. Biol. Chem.* **270,** 13392–13398
26. Michelotti, E. F., Sanford, S., Freije, J. M. P., MacDonald, N. J., Steeg, P. S., and Levens, D. (1997) *J. Biol. Chem.* **272,** 22526–22530

---

[3] F. Agou, unpublished results.

27. Wells, R. D. (1988) *J. Biol. Chem.* **263,** 1095–1098
28. Mirkin, S. M., Lyamichev, V. I., Drushlyak, K. N., Dobrynin, V. N., Filippov, S. A., and Frank-Kamenetskii, M. D. (1987) *Nature* **330,** 495–497
29. Simonsson, T., Pecinka, P., and Kubista, M. (1998) *Nucleic Acids Res.* **26,** 1167–1172
30. Albert, T., Mautner, J., Funk, J. O., Hortnagel, K., Pullner, A., and Eick, D. (1997) *Mol. Cell. Biol.* **17,** 4363–4371
31. Michelotti, E. F., Michelotti, G. A., Aronsohn, A. I., and Levens, D. (1996) *Mol. Cell. Biol.* **16,** 2656–2659
32. Hildebrandt, M., Lacombe, M.-L., Mesnildrey, S., and Veron, M. (1995) *Nucleic Acids Res.* **23,** 3858–3864
33. Sambrook, J., Fritsch, E. F., and Maniatis, T. (1989) *Molecular Cloning: A Laboratory Manual* 2nd Ed., Cold Spring Harbor Laboratory, Cold Spring Harbor, NY
34. Puglisi, J. D., and Tinoco, I., Jr. (1989) *Methods Enzymol.* **180,** 304–325
35. Karlsson, A., Mesnildrey, S., Xu, Y., Morera, S., Janin, J., and Veron, M. (1996) *J. Biol. Chem.* **271,** 19928–19934
36. Record, M. T., Jr., Lohman, M. L., and De Haseth, P. (1976) *J. Mol. Biol.* **107,** 145–158
37. Lohman, T. M., deHaseth, P. L., and Record, M. T., Jr. (1980) *Biochemistry* **19,** 3522–3530
38. Laue, T. M., Bhaivari, D. S., Ridgeway, T. M., and Pelletier, S. L. (1992) in *Analytical Ultracentrifugation in Biochemistry and Polymer Science* (Harding, S., Rowe, A. J., and Horton, J. C., eds), pp. 90–125, Royal Society of Chemistry Press, Cambridge, UK
39. Schaertl, S. (1996) *FEBS Lett.* **394,** 316–320
40. Webb, P. A., Perisic, O., Mendola, C. E., Backer, J. M., and Williams, R. L. (1995) *J. Mol. Biol.* **251,** 574–587
41. Mesnildrey, S., Agou, F., and Veron, M. (1997) *FEBS Lett.* **418,** 53–57
42. Flinta, C., Persson, B., Jornvall, H., and von Heijne, G. (1986) *Eur. J. Biochem.* **154,** 193–196
43. Postel, E. H., Mango, S. E., and Flint, S. J. (1989) *Mol. Cell. Biol.* **9,** 5123–5133
44. Ha, J. H., Spolar, R. S., and Record, M. T., Jr. (1989) *J. Mol. Biol.* **209,** 801–816
45. Schaertl, S., Konrad, M., and Geeves, M. A. (1998) *J. Biol. Chem.* **273,** 5662–5669
46. Schneider, B., Xu, Y., Sellam, O., Sarfati, R., Janin, J., Veron, M., and Deville-Bonne, D. (1998) *J. Biol. Chem.* **273,** 11491–11497
47. Woodbury, C. P., Jr., and von Hippel, P. H. (1983) *Biochemistry* **22,** 4730–4737
48. Postel, E. H., Weiss, V. H., Beneken, J., and Kirtane, A. (1996) *Proc. Natl. Acad. Sci. U. S. A.* **93,** 6892–6897
49. Battey, J., Moulding, C., Taub, R., Murphy, W., Stewart, T., Potter, H., Lenoir, G., and Leder, P. (1983) *Cell* **34,** 779–787
50. Levens, D., Duncan, R. C., Tomonaga, T., Michelotti, G. A., Collins, I., Davis-Smyth, T., Zheng, T., and Michelotti, E. F. (1997) *Curr. Top. Microbiol. Immunol.* **224,** 33–46
51. Tomonaga, T., and Levens, D. (1996) *Proc. Natl. Acad. Sci. U. S. A.* **93,** 5830–5835
52. Tomonaga, T., Michelotti, G. A., Libutti, D., Uy, A., Sauer, B., and Levens, D. (1998) *Mol. Cell* **1,** 759–764